Bull. Mater. Sci., Vol. 19, No. 3, June 1996, pp. 513–525. © Printed in India.

Effect of composition on dielectric and electrical properties of the $Sr_{1-x}La_xTi_{1-x}Co_xO_3$ system†

SHAIL UPADHYAY, DEVENDRA KUMAR* and OM PARKASH
School of Materials Science and Technology, *Department of Ceramic Engineering, Institute of Technology, Banaras Hindu University, Varanasi 221 005, India

Abstract. Valence compensated perovskite system $Sr_{1-x}La_xTi_{1-x}Co_xO_3$ shows dielectric relaxor behaviour with very high value of dielectric constant in the composition range $0{\cdot}20 < x < 0{\cdot}40$. In this paper the effect of composition on microstructure and the resulting electrical behaviour is reported. The compositions with $x = 0{\cdot}25, 0{\cdot}30, 0{\cdot}33, 0{\cdot}35$ and $0{\cdot}37$ have been synthesized by solid state ceramic method and dielectric measurements were made in the temperature range of 300–500 K and frequency range of 100 Hz to 1 MHz. Grain boundaries played an important role in their dielectric behaviour. Complex plane impedance and modulus techniques were used to separate out the contributions of grain and grain-boundaries to the resulting dielectric behaviour. It was observed that the bulk resistivity as well as the grain boundaries resistance decreased with increasing x. Furthermore, impedance analysis demonstrated that extremely high value of dielectric constant observed in these materials was due to barrier layers formation at grain–grain-boundaries interfaces.

Keywords. Dielectric properties; relaxor; impedance and modulus spectroscopy.

1. Introduction

Valence compensated perovskites of the type $A_{1-x}A'_xB_{1-x}B'_xO_3$ (where $A = Ca^{2+}$, Sr^{2+}, Ba^{2+}, Pb^{2+} or Na^{1+}; $A' = La^{3+}$, Nd^{3+}, Gd^{3+}; $B = Ti^{4+}$, Sn^{4+} or Nb^{5+}; $B' = Co^{+3}$, Ni^{+3}) have been studied extensively in the last ten years (Prasad 1988; Tiwari 1994). A few compositions in the system $Sr_{1-x}La_xTi_{1-x}Co_xO_3$ ($0{\cdot}20 < x < 0{\cdot}40$) exhibit interesting and useful dielectric properties (Parkash *et al* 1990). These materials exhibit a broad maxima in their dielectric constant vs temperature plots. The peak maxima shifts to higher temperature side with increasing frequency. These features are similar to those of the relaxor ferroelectrics (Newnham 1983; Cross 1987). The relaxor ferroelectrics (e.g. $PbMg_{1/3}Nb_{2/3}O_3$) contain random distribution of heterovalent ions (Mg^{2+} and Nb^{5+} in the above case) on B site of ABO_3 lattice. This gives rise to active ferroelectric regions interconnected by inactive non-ferroelectric regions. The statistical fluctuations in composition in these materials lead to large fluctuations in the Curie temperature of local regions. The broad maxima observed is the result of overlap of behaviour of all such regions. In relaxor ferroelectric materials, dielectric constant, ε_r, above peak maxima obeys the relation (Kirillov and Isupov 1973):

$$\frac{1}{\varepsilon_r} - \frac{1}{\varepsilon_{r\,max}} = \frac{(T - T_c)^2}{2\varepsilon_{r\,max}\delta^2},$$

where $\varepsilon_{r\,max}$ is the peak value of dielectric constant observed at T_c and δ a measure of the fluctuations in Curie temperature of local regions. Compositions in the system

†Paper presented at the poster session of MRSI AGM VI, Kharagpur, 1995

$Sr_{1-x}La_xTi_{1-x}Co_xO_3$ ($0{\cdot}20 < x < 0{\cdot}40$) obey this relation both above and below T_c (Parkash *et al* 1990). No direct evidence of ferroelectricity, however, is available at present.

These materials also exhibit unusual high values of dielectric constant. This has been ascribed to the formation of barrier layers at grain–grain boundaries interfaces. These materials are expected to lose traces of oxygen during sintering at high temperature according to the reaction:

$$O_0 \rightarrow 1/2O_2 + V_0^{\cdot\cdot} + 2e', \tag{1}$$

where all the species are written according to Kröger–Vink notation of defects. Electrons released in (1) make the materials semiconducting. During cooling of these samples after sintering, re-oxidation takes place. Due to decreasing temperature and insufficient time available for diffusion of oxygen to the bulk of material, reoxidation is limited to the surface and grain-boundaries. This makes grain-boundaries insulating as compared to the grains which still remain semiconducting. This difference in the conductivity of the grains and grain-boundaries gives rise to barriers at their interfaces imparting very high value of dielectric constant to the resulting ceramic. Thus, the overall dielectric behaviour of these materials has been proposed to have two contributions (i) one of ferroelectric nature in local microregions and (ii) other of interfacial polarization due to difference in the conductivity of grains and grain-boundaries as well as chemical microheterogeneities. The high value of dielectric constant in these materials makes them potential candidates for multilayer ceramic capacitors applications. Normally the manufacture of barrier layer materials based on $SrTiO_3$ requires, the firing of undoped or donor doped $SrTiO_3$ in a reducing atmosphere of H_2 at a very high temperature ($> 1400°C$) followed by cooling in an oxidizing atmosphere to develop barrier layers (Yamaoka 1986). The system under investigation exhibits barrier layers characteristics even on sintering in air at a much lower temperature (1250°C). Interesting and useful properties of these materials prompted us to study in detail the effect of composition on the dielectric and electrical properties of this system. With this in view a few more compositions in the range $0{\cdot}20 < x < 0{\cdot}40$ have been synthesized by solid state ceramic route and their electrical and dielectric properties are reported in this paper.

2. Experimental

Samples with $x = 0{\cdot}25$, $0{\cdot}30$, $0{\cdot}33$, $0{\cdot}35$ and $0{\cdot}37$ were prepared by the traditional ceramic method using $SrCO_3$, La_2O_3, $Co(C_2O_4)_2 2H_2O$ and TiO_2, all the chemicals with a purity above 99·5%. Appropriate quantities of these materials were weighed out accurately and ground in an agate mortar with acetone. The dried powders were calcined at 1475 K for 6 h and then furnace cooled. The resulting powders were ground and mixed with 2% polyvinyl alcohol and pressed as cylindrical pellets (dia. 12 mm) with an optimum load of 25 KN. The pellets were slowly heated up to 875 K and held at this temperature for 1 h to burn off the binder. Thereafter the temperature was raised to 1625 K, the pellets were sintered at this temperature for 6 h. The sintered pellets were reground, pelletized and sintered at 1625 K further for 18 h.

Powder X-ray diffraction patterns were recorded for the sintered samples using diffractometer (Rigaku RU-200 B Series). For the measurements of dielectric properties, the sintered pellets were polished and washed with isopropanol to remove any moisture.

Air-dried silver paint was used for electroding the samples. Capacitance, dielectric loss and conductance were measured as a function of temperature (300–500 K) in the frequency range of 100 Hz–1 MHz using Hewlett–Packard 4129A LF Impedance Analyzer. Micrographs of the etched and coated samples were observed using Jeol PSM 800 scanning electron microscope (SEM).

3. Results and discussion

X-ray powder diffraction (XRD) patterns of all the sintered samples obtained confirmed the formation of single phase solid solution. Absence of characteristic lines of the constituent oxides indicated the formation of single phase in all the compositions. XRD data of all the compositions were indexed on the basis of cubic unit cell similar to undoped $SrTiO_3$ (Parkash *et al* 1989). The lattice parameter '*a*' for various compositions is given in table 1. The lattice parameter '*a*' decreases with increasing *x*. This can be explained in terms of the ionic sizes of Sr^{2+} (1·44 Å), La^{3+} (1·32 Å), Ti^{4+} (0·605 Å) and Co^{3+} (high spin state $t_{2g}^4e_g^2$, 0·61 Å; low spin state $t_{2g}^6e_g^0$, 0·525 Å) respectively. La^{3+} and Sr^{2+} ions have different ionic sizes. Because of the smaller ionic size of La^{3+} than that of Sr^{2+}, lattice parameter decreases with increasing *x*. Besides the smaller ionic size of La^{+3}, cobalt ions are known to exist in low as well as high spin states in $LaCoO_3$ (Raccah and Goodenough 1967; Bhide *et al* 1972). The presence of low spin cobalt ions in these samples may also decrease the lattice parameter with increasing *x*. Percentage porosity for all the compositions are given in table 1. Table 1 shows that there is not a significant change in porosity for the different samples. The bulk density of all the samples is > 90% of the theoretical density. Sinterability is being maximum for the composition with $x = 0{\cdot}35$.

SEM of the polished and chemically etched surfaces of the compositions with $x = 0{\cdot}25$, 0·33 and 0·37 are shown in figure 1. The average grain size calculated by the line intercept method is given in table 1. It can be noted that the average grain size for $x = 0{\cdot}25$ and 0·30 samples is small (2–3 μm) while that of the samples with $x = 0{\cdot}33$, 0·35 and 0·37 is considerably large (8 μm).

All the samples exhibit an anomaly in the variation of their dielectric constant, ε_r, with temperature. Typical variation of dielectric constant, ε_r, and dissipation factor, *D*, (for composition with $x = 0{\cdot}37$) with temperature at frequencies, 1 KHz, 10 KHz and 100 KHz is shown in figure 2. Dielectric behaviour of the other compositions are similar to this composition. Room temperature ε_r, T_c and $\varepsilon_{r\,max}$ at three different

Table 1. Lattice parameter, percentage porosity and average grain size for different compositions in the system $Sr_{1-x}La_xTi_{1-x}Co_xO_3$.

Composition *x*	Lattice parameter (Å)	Porosity (%)	Average grain size (μm)
0·25	3·887	3	1
0·30	3·886	5	3
0·33	3·883	9	8
0·35	3·881	4	7
0·37	3·877	10	8

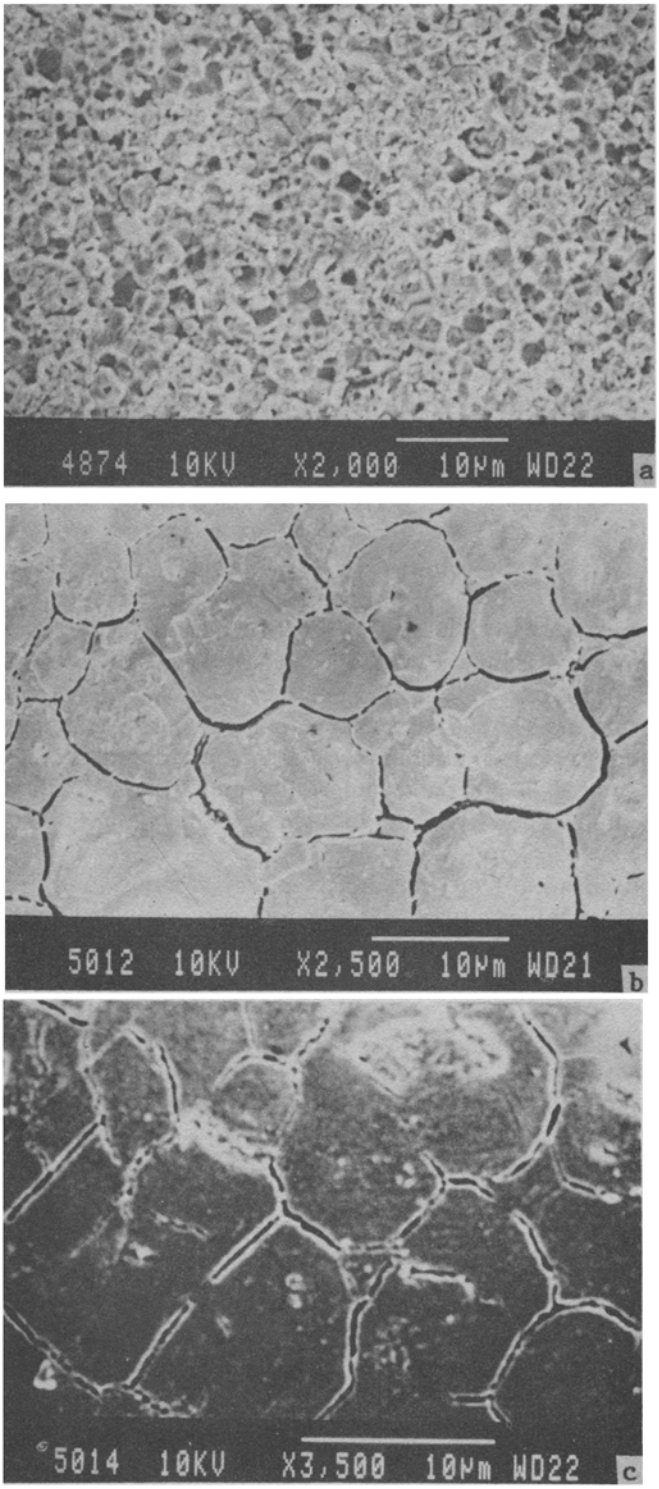

Figure 1. SEM micrographs of the samples in the $Sr_{1-x}La_xTi_{1-x}Co_xO_3$ system: (**a**) $x = 0{\cdot}25$, (**b**) $x = 0{\cdot}33$ and (**c**) $x = 0{\cdot}37$.

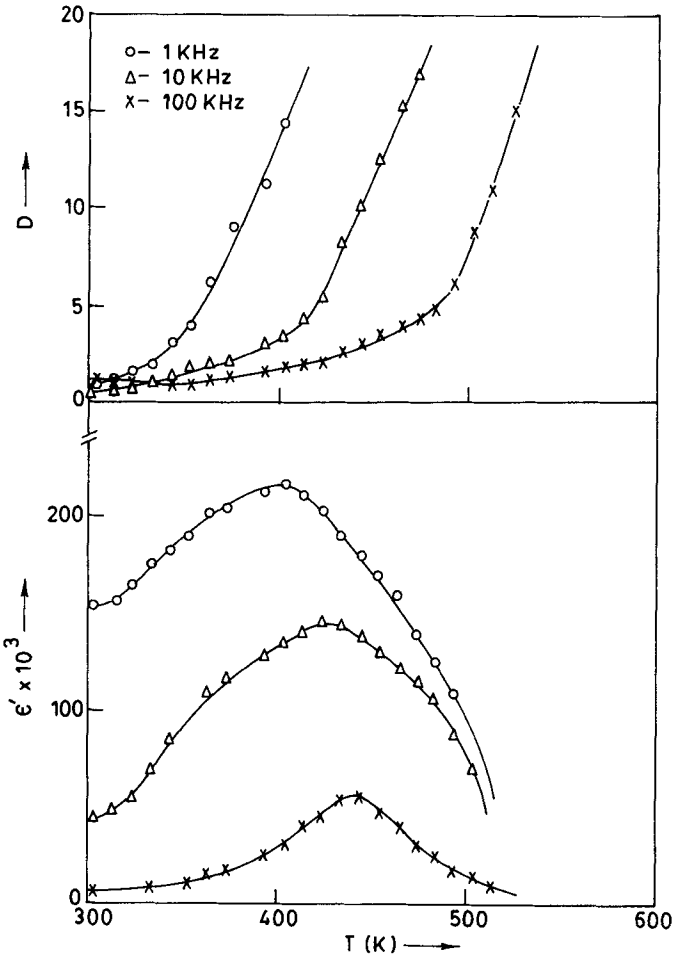

Figure 2. Variation of dielectric constant ε_r and dissipation factor D with temperature for the composition $Sr_{0.63}La_{0.37}Ti_{0.63}Co_{0.37}O_3$.

frequencies 1 KHz, 10 KHz and 100 KHz for all the compositions are given in table 2. From the study of all the compositions, it is noted that the dielectric constant increases with increasing x. It becomes maximum for the composition with $x = 0{\cdot}35$ attaining a value of $1{\cdot}9 \times 10^5$ at room temperature at 1 KHz. This is about three orders of magnitude higher than undoped $SrTiO_3$ for which ε_r is 300 at 1 KHz at room temperature. It is observed from table 2 that the temperature, T_c at which ε_r shows a maximum value, $\varepsilon_{r\,max}$ shifts to the higher temperature side with increasing frequency. The value of ε_r itself decreases with increasing frequency, the decrease being more pronounced near T_c for all the samples. These features are similar to relaxor ferroelectrics as mentioned in the introduction. In relaxor ferroelectrics, heterovalent ions are randomly distributed on octahedral sites. This gives rise to ferroelectric regions which are interconnected by non-ferroelectric regions. On cooling these materials, these ferroelectric microregions grow in size. Due to statistical fluctuations in the compositions in these micro-regions, different regions will have different Curie temperatures. The overall behaviour of material is the broad envelope of behaviour of these different

Table 2. Values of T_c, ε_{rmax} and ε_{rRT} at three frequencies 1, 10, 100 KHz for different compositions in the $Sr_{1-x}La_xTi_{1-x}Co_xO_3$ system.

Composition x	T_c(K)			$\varepsilon'_{rmax}10^3$			$\varepsilon_{rRT}10^3$		
	1 KHz	10 KHz	100 KHz	1 KHz	10 KHz	100 KHz	1 KHz	10 KHz	100 KHz
0·25	433	495	540	2	1	0·4	0·6	0·4	0·2
0·30	426	483	538	72	30	7·5	4·2	0·8	0·4
0·33	423	463	513	78	34	10·0	5·8	5·7	3·4
0·35	413	443	454	340	210	91·4	187·2	54·4	7·3
0·37	403	428	443	220	146	56·2	154·0	39·0	4·2

regions resulting in a broad maxima in ε_r vs T plots. System $Sr_{1-x}La_xTi_{1-x}Co_xO_3$ has been prepared by solid state ceramic route. Due to the slow diffusion of ions in this thermochemical process the resulting materials are expected to contain chemical microheterogeneities. These microheterogeneities arise due to random occupation of A and B sites of ABO_3 perovskite lattice by La^{3+} or Sr^{2+} and Co^{3+} or Ti^{4+} ions respectively. There may be local regions having deviation from cubic symmetry because of heterovalent substitutions even though the overall symmetry remains cubic. These distortions in local regions will give rise to ferroelectricity in them. Thus we have local ferroelectric regions interconnected via non-ferroelectric matrix. Because of random occupation of equivalent sites by different heterovalent ions, there are statistical fluctuations in the compositions of these regions. Therefore, different regions will have different Curie temperature and hence the broadening of the peak observed in ε_r vs T plots. Further, because of the different compositions of different micro-regions (ferroelectric as well as non-ferroelectric) their conductivities will be different. This gives rise to interfacial polarization. This is reflected in the sharp fall of dielectric constant of all the samples in the frequency range 100 Hz –10 KHz.

Unusual high values of dielectric constant ($> 10^5$) observed in some of these compositions is because of the formation of barrier layers at grain–grain-boundaries interfaces as discussed in the introduction. In barrier layer materials, the apparent dielectric constant depends almost linearly on the grain size according to an empirical formula (Yamaoka 1986)

$$\varepsilon_{s,app} = (0{\cdot}115G_s + 0{\cdot}40) \times 10^4, \tag{2}$$

where

G_s = grain size.

Thus, larger grain size gives higher value of dielectric constant. Samples with $x = 0{\cdot}33$, 0·35 and 0·37 having large grain size have been found to have higher values of dielectric constant as compared to the small grain sized samples with $x = 0{\cdot}25$ and 0·30. This is in accordance with relation (2).

The formation of barrier layers is confirmed by impedance analysis. The overall electrical properties of a polycrystalline ceramic solid has contribution from grains, grain boundaries and solid electrode interfaces. Each of these contributions can be represented by a suitable combination of resistance and capacitance in parallel. The sample can thus be represented by an equivalent circuit containing three parallel R–C

elements connected in series (Macdonald 1987). In impedance analysis, the imaginary part of the total complex impedance, Z^*, is plotted as a function of real part, Z' over a range of frequencies (10^2–10^6 Hz in our case). If the time constant for three RC elements is different (ratio > 10), each parallel RC element gives rise to a semicircle with its centre on the Z' axis if there is only single value of relaxation time (Pandey *et al* 1995). Resistance value for each element is obtained from the intercept of the arc on Z' axis corresponding to that element. Capacitance values are calculated by using the relation $\omega RC = 1$, where $\omega = 2\pi f$, f being the frequency corresponding to the maximum of each circular arc. If any of the above processes have a distribution of relaxation times, then one obtains a depressed circular arc in the impedance plot having its centre below the Z' axis.

Typical impedance plots of all the compositions at room temperature are shown in figure 3. Two depressed circular arcs have been observed in all the compositions except the composition with $x = 0{\cdot}25$. It will be discussed later that single arc for the composition with $x = 0{\cdot}25$ also represents two contributions. The lower frequency arc is assigned to the grain boundaries while the high frequency arc to the grains. There is no contribution from the electrode-specimen interface. This was confirmed by applying varying DC voltages and observing that resulting current was independent of time.

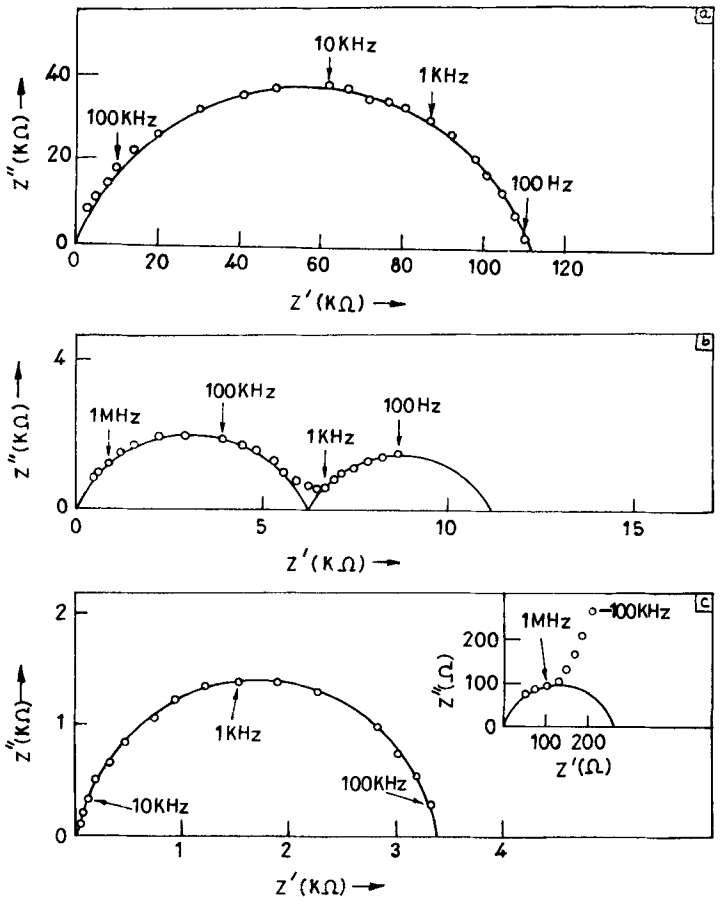

Figure 3.

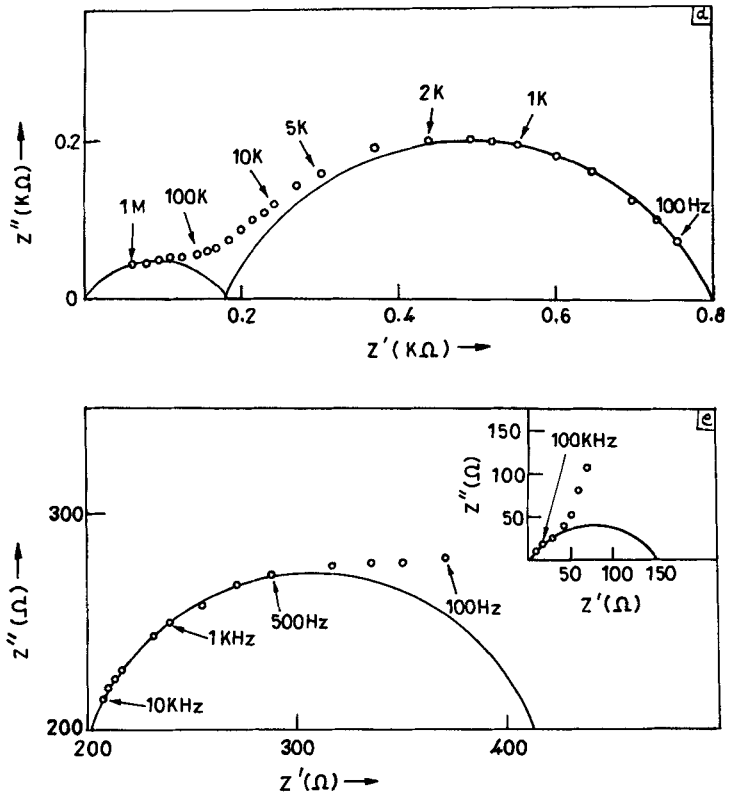

Figure 3. Complex impedance Z'' vs Z' plots at room temperature for different compositions (**a**) $x = 0{\cdot}25$, (**b**) $x = 0{\cdot}30$, (**c**) $x = 0{\cdot}33$, (**d**) $x = 0{\cdot}35$ and (**e**) $x = 0{\cdot}37$, in the $Sr_{1-x}La_xTi_{1-x}Co_xO_3$ system.

Table 3. Room temperature resistance and capacitance values of grains and grain-boundaries of different compositions obtained from impedance and modulus plots.

	Resistance		Capacitance	
Composition x	Grains, $R_g(\Omega)$/ resistivity (Ω–cm)	Grain boundaries $R_{gb}(\Omega)$	Grains, $C_g(pF)$/ ε_{rb}	Grain boundaries $C_{gb}(nF)$
0·25	$3{\cdot}1 \times 10^3/3{\cdot}2 \times 10^5$	$5{\cdot}5 \times 10^4$	73/319	073
0·30	$5{\cdot}0 \times 10^3/2{\cdot}1 \times 10^4$	$5{\cdot}2 \times 10^3$	155/415	320
0·33	$3{\cdot}0 \times 10^3/1{\cdot}8 \times 10^3$	$2{\cdot}5 \times 10^3$	640/1807	110
0·35	$6{\cdot}0 \times 10^2/3{\cdot}4 \times 10^2$	$1{\cdot}9 \times 10^2$	1140/2280	135
0·37	$5{\cdot}0 \times 10^2/3{\cdot}1 \times 10^2$	$1{\cdot}5 \times 10^2$	1061/1812	150

This showed absence of any electrode polarization. Resistance and capacitance of the grains and grain boundaries obtained from impedance plots for all the compositions are given in table 3. It is noted that both the bulk resistivity, ρ_b, and total grain-boundaries resistance, R_{gb}, decrease with increasing x, i.e. increasing cobalt ions concentration. This suggests that conduction is mainly due to cobalt ions as all the

other ions have inert gas configurations and as such are not expected to participate in the conduction. The bulk resistivity values decreases by about three orders of magnitude in increasing x from 0·25 to 0·37. The value of bulk dielectric constant also increases on increasing x. This may be due to increase in the volume fraction of ferroelectric microregions with increasing x as expected. Table 3 shows that the capacitance associated with the grain-boundaries is about two to three orders of magnitude higher than that of the bulk for all the compositions except the composition with $x = 0{\cdot}25$ where two capacitances are almost equal. The difference in capacitance value is due to the formation of barrier layers at grain-boundaries which is not observed in the sample with $x = 0{\cdot}25$, that is why dielectric constant value of this sample is small as compared to all the other compositions.

Complex plane modulus plots give complementary information to the information given by complex plane impedance plots. The modulus data are calculated in the form of imaginary part of modulus, M'' and real part, M' by using the relations, $M' = \omega C_0 Z''$ and $M'' = \omega C_0 Z'$ (ω, is angular frequency $= 2\pi f$ and C_0 the vacuum capacitance of the measuring cell and electrodes with an air gap in place of the sample). The impedance plots highlight the most resistive element whereas modulus plots the least capacitive part of the equivalent R–C circuit (Hodge *et al* 1976; Sinclair and West 1989). In modulus plots intercept of circular arc on the real axis, i.e. on M' axis is given by C_0/C (varies inversely with the capacitance). Typical modulus plots of these samples at room temperature are shown in figure 4. Except $x = 0{\cdot}30$, in all other compositions, two circular arcs have been observed. The low frequency arc is assigned to the grain boundaries while high frequency arc to the grains. Composition with $x = 0{\cdot}30$, only one arc is observed because of a marked difference in the capacitance of the grains and grain boundaries ($C_{gb} = 2000 \times C_b$). The arc corresponding to the grain boundaries has been

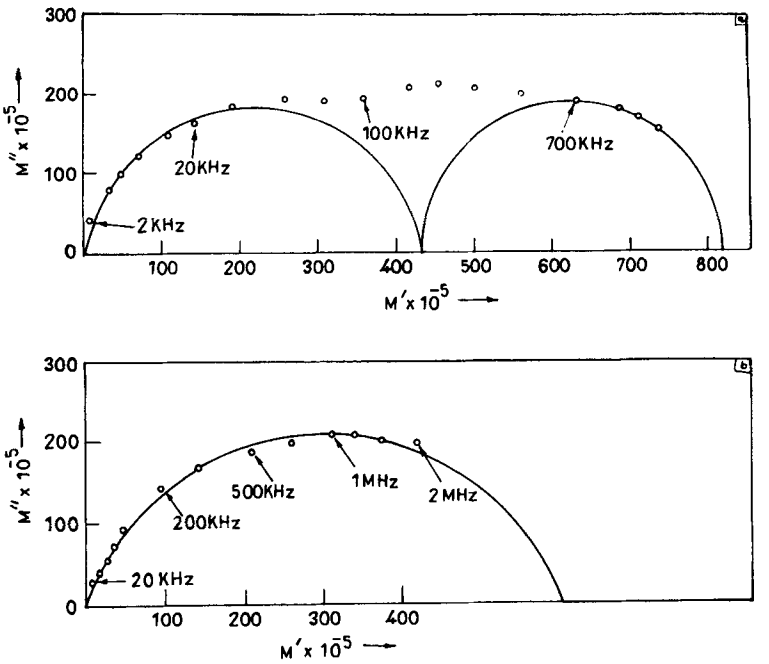

Figure 4.

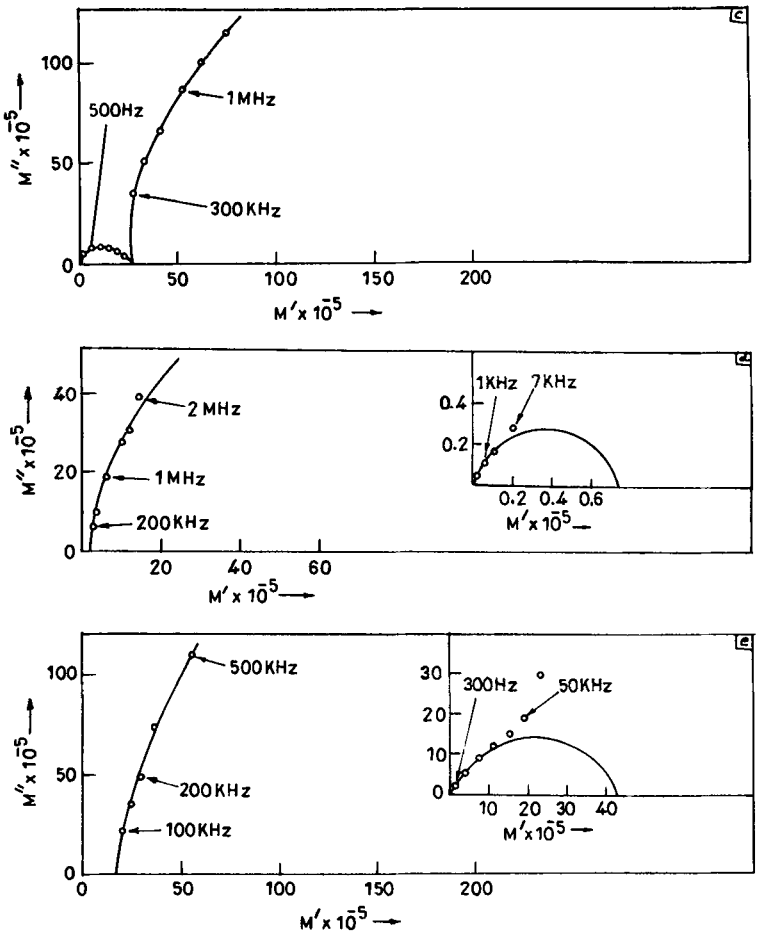

Figure 4. Complex modulus M'' vs M' plots for different compositions at room temperature: (**a**) $x = 0{\cdot}25$, (**b**) $x = 0{\cdot}30$, (**c**) $x = 0{\cdot}33$, (**d**) $x = 0{\cdot}35$ and (**e**) $x = 0{\cdot}37$, in the $Sr_{1-x}La_xTi_{1-x}Co_xO_3$ system.

suppressed and only one arc corresponding to the grains is seen in this sample. For the composition with $x = 0{\cdot}25$, the capacitance of the grains and grain boundaries is almost equal; that is why two arcs are observed. From the modulus plot of this composition resistance value of grain and grain-boundaries are obtained and is given in table 3. The table shows that the resistance of grain-boundaries is larger as compared to the grains by about two orders of magnitude. That is why the arc corresponding to grains is suppressed in the complex plane impedance plot of this composition. Larger value of grain boundaries resistance in this sample is ascribed to large volume occupied by grain-boundaries resulting from small grain size in this sample. Whereas in other three compositions with $x = 0{\cdot}33$, $0{\cdot}35$ and $0{\cdot}37$ two circular arcs are seen but it is noted that capacitance of the grains and grain boundaries are considerably different in these samples (table 3).

The values of resistance of grains and grain boundaries were found from the impedance plots for all the compositions except the composition with $x = 0{\cdot}25$ in which these were obtained from the modulus plots. Plots of the logarithm of resistance of the grains and grain boundaries as a function of inverse temperature ($1000/T$) are shown in

figure 5. These plots are linear showing that resistance/resistivity obeys an Arrhenius relationship

$$\rho = \rho_0 \exp(E_a/RT),$$

where E_a is the activation energy for conduction. Values of activation energies obtained by least square fitting of the data are given in table 4. It is noted that the value of activation energy of conduction, both for grains, E_g, and grain-boundaries, E_{gb} are similar and decrease with increasing x. Similar values of activation energies of conduction for grains and grain-boundaries show that mechanism of conduction is the same in both the cases. Though the activation energies for grain-boundaries are almost similar yet they are higher than those for the bulk of all the compositions. This may be due to more disorder present in the grain-boundaries. $SrTiO_3$ is a wide band gap material, similar to TiO_2 in which the filled valence band comprised of oxygen $2p$ orbitals is separated from the empty conduction band of Ti $4s$ orbitals by 3·0 eV

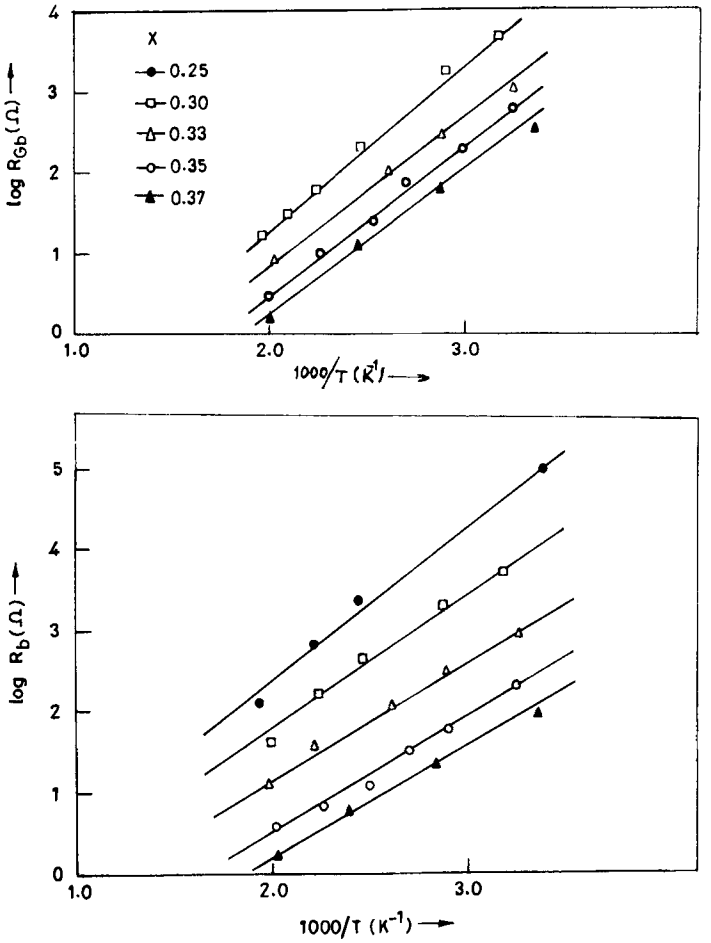

Figure 5. Variation of logarithm of grains and grain boundaries resistance (R_g and R_{gb}) with inverse of temperature in the $Sr_{1-x}La_xTi_{1-x}Co_xO_3$ system.

Table 4. Activation energies of conduction E_g (grain) and E_{gb} (grain-boundaries) for various samples in the system $Sr_{1-x}La_xTi_{1-x}Co_xO_3$.

Compositions x	E_g(eV)	E_{gb}(eV)
0·25	0·39	0·42
0·30	0·32	0·41
0·33	0·28	0·35
0·35	0·28	0·35
0·37	0·25	0·34

(Grandy 1959; Eror and Balachandran 1982). Obtained values of activation energies rule out the possibility of intrinsic conduction in these materials. It has been reported that Co^{3+} gives rise to energy levels at 0·70 eV above the valence band (Mizushima *et al* 1972). The conduction therefore seems to occur through Co^{2+} and Co^{3+} ions. Generation of Co^{2+} ions can be explained as follows. These materials are expected to lose traces of oxygen during their firing at high temperature (1). In this process electrons are released, these electrons may be either captured by Ti^{4+} or Co^{3+} ions to produce Ti^{3+} or Co^{2+} ions respectively. The Ti^{4+} ion, with inert gas configuration represents the most stable state of the titanium ion in air. Thus, the probability of generation of Ti^{3+} ions is small and present system may contain small amounts of divalent cobalt ions. The conduction in these materials seem to occur through hopping of charge carriers among localized Co^{2+} and Co^{3+} sites. This is in accordance with the decreasing value of activation energies of conduction with increasing x (Karim *et al* 1979).

4. Conclusions

Dielectric and electrical properties of this system depend on the composition i.e. x. Resistivity and activation energies of conduction decreases with increasing x, indicating that conduction occurs mainly due to cobalt ions. Value of bulk dielectric constant increases with increasing x. This has been attributed to the increase in the volume fraction of ferroelectric micro-regions arising due to random heterovalent substitution. Extremely high value of dielectric constant has been explained in terms of the barrier layer formation at the grain–grain-boundaries interfaces.

Acknowledgements

The authors thank the Department of Science and Technology, Government of India for financial support. One of the authors (SU) also thanks UGC for providing research fellowship.

References

Bhide V G, Rajoria D S, Rao G R and Rao C N R 1972 *Phys. Rev.* **B6** 1021
Cross L E 1987 *Ferroelectrics* **76** 241
Eror N G and Balachandran U 1982 *J. Am. Ceram. Soc.* **65** 426

Grandy H W 1959 *Phys. Rev.* **113** 795
Hodge I M, Ingram M D and West A R 1976 *J. Electroanal. Chem.* **74** 125
Karim D P and Aldred A T 1979 *Phys. Rev.* **B20** 2255
Kirillov V V and Isupov V A 1973 *Ferroelectrics* **5** 3
Macdonald J R 1987 *Impedance spectroscopy* (New York: John Wiley Sons) ch. IX
Mizushima K, Tanaka M and Iida S 1972 *J. Phys. Soc. Jap.* **32** 1519
Newnham R E 1983 *J. Mater. Educ.* **5** 94
Pandey L, Parkash O, Rajesh K K and Kumar D 1995 *Bull. Mater. Sci.* **18** 5
Parkash O, Prasad Ch D and Kumar D 1989 *Phys. Status Solidi (a)* **116** K81
Parkash O, Prasad Ch D and Kumar D 1990 *J. Mater. Sci.* **25** 487
Prasad Ch D 1988 *Studies of electrical properties of perovskite oxide* $M_{1-x}La_xTi_{1-x}Co_xO_3$ *(M = Pb, Ba, Sr and Ca)*, Ph D Thesis, Banaras Hindu University, Varanasi
Raccah P M and Goodenough J B 1967 *Phys. Rev.* **155** 932
Sinclair D C and West A R 1989 *J. Appl. Phys.* **66** 3850
Tiwari H S 1994 *Dielectric and electrical properties of some valence compensated oxide perovskite*, Ph D Thesis, Banaras Hindu University, Varanasi
Xue L A, Chen Y and Brook R J 1988 *J. Mater. Sci.* **7** 1163
Yamaoka N 1986 *Bull. Am. Ceram. Soc.* **65** 1149